J. Gen. Appl. Microbiol., **66**, 106–115 (2020)
doi 10.2323/jgam.2019.11.008

jGAM

Full Paper

Acclimation process of the chlorophyll *d*-bearing cyanobacterium *Acaryochloris marina* to an orange light environment revealed by transcriptomic analysis and electron microscopic observation

(Received September 30, 2019; Accepted November 29, 2019; J-STAGE Advance publication date: March 7, 2020)

Tomonori Kashimoto,[1] Keita Miyake,[1] Mayuko Sato,[2] Kaisei Maeda,[3,4] Chikahiro Matsumoto,[1] Masahiko Ikeuchi,[3,5] Kiminori Toyooka,[2] Satoru Watanabe,[4] Yu Kanesaki,[6,7,*] and Rei Narikawa[1,5,6,*]

[1] *Department of Biological Science, Faculty of Science, Shizuoka University, Ohya, Suruga-ku, Shizuoka 422-8529, Japan*
[2] *RIKEN Center for Sustainable Resource Science, Suehiro-cho, Tsurumi-ku, Yokohama 230-0045, Japan*
[3] *Department of Life Sciences (Biology), Graduate School of Arts and Sciences, The University of Tokyo, Komaba, Meguro, Tokyo 153-8902, Japan*
[4] *Department of Bioscience, Tokyo University of Agriculture, Sakuragaoka, Setagaya-ku, Tokyo 156-8502, Japan*
[5] *Core Research for Evolutional Science and Technology, Japan Science and Technology Agency, Honcho, Kawaguchi, Saitama 332-0012, Japan*
[6] *Research Institute of Green Science and Technology, Shizuoka University, Ohya, Suruga-ku, Shizuoka 422-8529, Japan*
[7] *NODAI Genome Research Center, Tokyo University of Agriculture, Sakuragaoka, Setagaya-ku, Tokyo 156-8502, Japan*

The cyanobacterium *Acaryochloris marina* MBIC 11017 (*A. marina* 11017) possesses chlorophyll *d* (Chl. *d*) peaking at 698 nm as photosystem reaction center pigments, instead of chlorophyll *a* (Chl. *a*) peaking at 665 nm. About 95% of the total chlorophylls is Chl. *d* in *A. marina* 11017. In addition, *A. marina* 11017 possesses phycobilisome (PBS) supercomplex to harvest orange light and to transfer the absorbing energy to the photosystems. In this context, *A. marina* 11017 utilizes both far-red and orange light as the photosynthetic energy source. In the present study, we incubated *A. marina* 11017 cells under monochromatic orange and far-red light conditions and performed transcriptional and morphological studies by RNA-seq analysis and electron microscopy. Cellular absorption spectra, transcriptomic profiles, and microscopic observations demonstrated that PBS was highly accumulated under an orange light condition relative to a far-red light condition. Notably, transcription of one *cpcBA* operon encoding the phycobiliprotein of the phycocyanin was up-regulated under the orange light condition, but another operon was constitutively expressed under both conditions, indicating functional diversification of these two operons for light harvesting. Taking the other observations into consideration, we could illustrate the photoacclimation processes of *A. marina* 11017 in response to orange and far-red light conditions in detail.

Key Words: cyanobacteriochrome; cyclic electron transport; plasmid; rod-membrane linker

Introduction

Cyanobacteria are prokaryotes that perform oxygenic photosynthesis, almost the same as chloroplasts of the land plants. Cyanobacteria possess photosystem I (PS I) and photosystem II (PS II) that organize a linear electron transport chain in corporation with cytchrome b_6f. Because most PS I and PS II bind chlorophyll *a*, these photosynthetic apparatuses utilize blue and red light regions for the en-

*Corresponding author: Yu Kanesaki[1] and Rei Narikawa[2], [1]Research Institute of Green Science and Technology, Shizuoka University, Ohya, Suruga-ku, Shizuoka 422-8529, Japan; [1]NODAI Genome Research Center, Tokyo University of Agriculture, Sakuragaoka, Setagaya-ku, Tokyo 156-8502, Japan; [2]Department of Biological Science, Faculty of Science, Shizuoka University, Ohya, Suruga-ku, Shizuoka 422-8529, Japan; [2]Core Research for Evolutional Science and Technology, Japan Science and Technology Agency, Honcho, Kawaguchi, Saitama 332-0012, Japan; [2]Research Institute of Green Science and Technology, Shizuoka University, Ohya, Suruga-ku, Shizuoka 422-8529, Japan.
[1]Tel: +81-54-238-4385 E-mail: kanesaki.yuh@shizuoka.ac.jp; [2]Tel: +81-54-238-4783 E-mail: narikawa.rei@shizuoka.ac.jp

None of the authors of this manuscript has any financial or personal relationship with other people or organizations that could inappropriately influence their work.

ergy source. Most cyanobacteria possess a phycobilisome light-harvesting supercomplex (PBS) that preferentially transfers energy to PS II under normal light conditions (Watanabe and Ikeuchi, 2013). Because the PBS absorbs a wide visible region from teal to red, cyanobacteria can utilize almost the full visible region for photosynthesis and, hence, is adapted to various aquatic and terrestrial environments. Compositions of PBS light-harvesting pigments are highly diversified depending on their habitats and species. The PBS is divided into two structural components, rod and core. The rod components are especially diversified because of their light-harvesting functions, whereas the core structure is composed of allophycocyanin subunits and is rather universal among various cyanobacteria because of their energy transferring functions.

PS I and PS II photosynthetic apparatuses are almost homogeneous regarding the binding chromophores. Recent studies, however, have revealed that two photosynthetic systems utilizing a red-shifted light source have been reported: inducible and constitutive systems (Gan and Bryant, 2015). The inducible system utilizes chlorophyll *f* as a photosynthetic pigment peaking at 706 nm (Chen et al., 2010). The chlorophyll *f* specifically accumulates under far-red light conditions, whereas only chlorophyll *a* accumulated under normal white light conditions (Chen et al., 2012). About 10% of the total chlorophyll is occupied by chlorophyll *f* under far-red light conditions. This chlorophyll *f* is suggested to function as antenna pigments, but not as reaction center pigments. This inducible system was widely distributed among various cyanobacteria, including phylogenetically distant species, indicating that this system has an anciently acquired character. In contrast, the constitutive system is restricted to only *Acaryochloris* genus to date and utilizes chlorophyll *d* as main photosynthetic pigments peaking at 698 nm (Miyashita et al., 1996). About 95% of the total chlorophyll is occupied by chlorophyll *d*. The chlorophyll *d* has been revealed to function as both antenna and reaction center pigments, which also contrasts with the situation for the chlorophyll *f*.

The detailed molecular mechanism of chlorophyll *f* induction has been revealed and is known as "Far-Red Light Photoacclimation (FaRLiP)" regulation (Gan et al., 2014). The phytochrome and its downstream regulators, RfpA/B/C, transcriptionally regulate many photosynthetic genes in the red/far-red reversible manner, and so photosynthetic apparatuses show a drastic conversion in response to far-red light illumination (Gan et al., 2014; Zhao et al., 2015). On the other hand, because chlorophyll *d* is constitutively accumulated in the *Acaryochloris* cells, specific regulation of chlorophyll *d* accumulation is not likely to be present in *Acaryochloris*. To date, genomic information of two species of *Acaryochloris* genus, *Acaryochloris marina* MBIC 11017 (*A. marina* 11017) and *Acaryochloris* sp. CCMEE 5410 (*A*. 5410) are available as complete and draft genome sequences, respectively (Swingley et al., 2008; Yoneda et al., 2016). Notably, *A. marina* 11017 possesses the PBS to harvest light energy in the orange region as well as other cyanobacteria, whereas *A*. 5410 has been reported to lack the PBS components (Miller et al., 2005; Yoneda et al., 2016). Furthermore, it has been reported that the PBS of *A. marina* 11017 consists of only the rod structure and lacks the core component (Chen et al., 2009). Cyanobacterium *Anabaena* sp. PCC 7120 has been shown to have a similar PBS composed of only the rod component to specifically transfer the light energy to PS I (Watanabe et al., 2014). To transfer the energy to PS I directly from the rod component, CpcL, which is a homolog of the rod-core linker CpcG, serves as a rod-membrane linker. CpcL possesses one membrane-associated region at the C-terminus, which may assist the energy transfer directly from the rod component. Interestingly, *A. marina* 11017 has membrane-associated CpcL homologs, but not canonical CpcG homologs (Watanabe and Ikeuchi, 2013), indicating that the PBS composed of only the rod component from *A. marina* 11017 also transfer the absorbing energy directly to photosynthetic reaction centers via the CpcL homologs.

Cyanobacteria possess various photoreceptors to acclimate to changing light environments. Among them, cyanobacteriochrome photoreceptors play central roles in these acclimation processes, such as phototactic regulation, chromatic acclimation and light-dependent cell aggregation (Enomoto et al., 2014, 2015; Hirose et al., 2010; Kehoe and Grossman, 1996; Narikawa et al., 2011; Savakis et al., 2012; Song et al., 2011; Wiltbank and Kehoe, 2016; Yang et al., 2018; Yoshihara et al., 2000). The cyanobacteriochrome photoreceptors bind linear tetrapyrrole chromophores, such as phycocyanobilin (PCB) and phycoviolobilin, and sense light quality and/or intensity information covering a wide range of light wavelengths from ultraviolet to far-red (Fushimi and Narikawa, 2019). Recently, we identified that several cyanobacteriochromes from *A. marina* 11017 bind biliverdin chromophore and reversibly photoconvert between a far-red absorbing form and an orange absorbing form (Fushimi et al., 2016, 2019; Narikawa et al., 2015). This finding indicates that *A. marina* 11017 possesses far-red/orange reversible photoacclimation processes. Because far-red and orange light sources are absorbed by photosystems and PBS, respectively, the far-red/orange reversible photoreceptors may be involved in chromatic acclimation processes of these photosynthetic apparatuses.

In the present study, we incubated *A. marina* 11017 cells under monochromatic orange or far-red light conditions and performed transcriptional and morphological studies by RNA-seq analysis and electron microscopy.

Materials and Methods

A. marina 11017 cultivation and spectroscopy. The original strain of *A. marina* 11017 was obtained from NITE Biological Research Center. The cyanobacterium *A. marina* 11017 was cultured at 25°C in IMK medium under continuous illumination provided by white fluorescent lamp (FL20SBR-A, NEC, Japan), orange (λ_{max} = 593 nm, half width = 7 nm) LED or far-red ((λ_{max} = 729 nm, half width = 8 nm) LED (VBP-L24-C2, Varol, Japan) with a light intensity of 10 μmol photons m^{-2} s^{-1} according to previous studies (Duxbury et al., 2009; Watabe et al., 2015), and bubbled with air. Culture absorbance was moni-

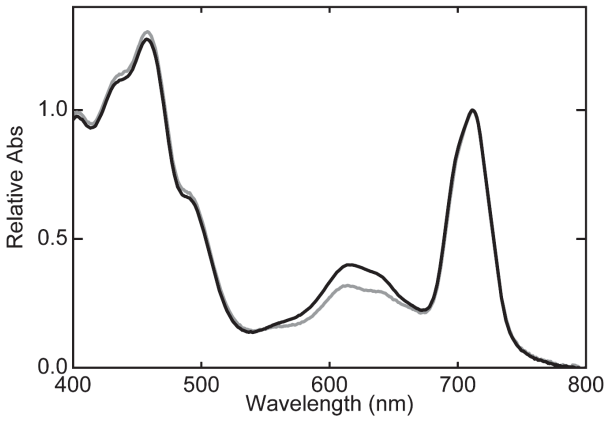

Fig. 1. Cellular absorption spectra. Cells under far-red (FRL, gray line) and orange (OL, black line) light conditions for 14 days.

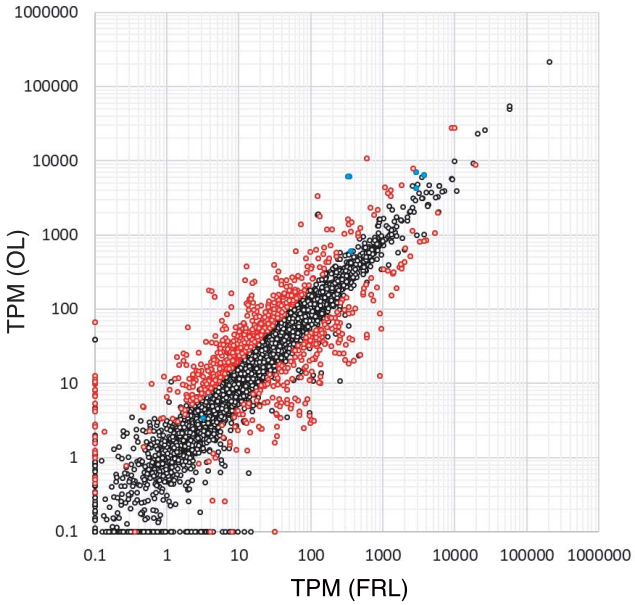

Fig. 2. Scatter-plot of RNA-seq transcriptome profiles.

TPM values of each gene are indicated. Cells were transferred from white light to far red light (FRL) or orange light (OL) for 1 h (See materials and methods). Red spots indicate the significant genes with a *P*-value less than 0.01, and with more than 2-fold changes of expression level. Blue spots indicate the genes for phycocyanin subunits. The other black spots indicate the non-significant genes with a *P*-value more than 0.01, and with less than 2-fold changes of expression level.

tored at 780 nm. Cellular absorbance spectra were monitored by a spectrophotometer equipped with an integrating sphere (UV-2600 & ISR-2600 Plus, Shimazu, Japan).

RNA isolation. Log-phase cells ($OD_{780} \approx 0.4$–1.0) under a white light condition were subcultured with a starting OD_{780} of 0.4 in a fresh medium under a dim white light condition (1 μmol photons m^{-2} s^{-1}) for 12 h. Next, cells were cultured under an orange or far-red light condition (10 μmol photons m^{-2} s^{-1}) for 1 h. After that, cell collection and disruption was performed under a dark condition on ice. After cell cultures were soaked in liquid N_2 to a non-freezing extent, the cells were collected by centrifugation at 20,400 × *g* for 10 min at 4°C. After removal of supernatants, the cell pellets were soaked in liquid N_2 to freeze. The frozen cell pellets were disrupted with a ballet bead (SK-100-DLC10, Tokken, Japan) by using a bead beater (MS-100R, TOMY, Japan). The bead-beating at 2,000 rpm for 20 s was performed six times with an interval of 20 s on ice. The disrupted cell pellets were mixed with 100 μL MilliQ water and 500 μL Plant RNA Reagent (Thermo Fisher Scientific, MA, USA). After 5 min incubation, an insoluble fraction was removed by centrifugation (12,000 × *g*, 2 min, room temperature). From the soluble fraction, nucleic acids were purified by the standard protocol of isopropyl alcohol precipitation and phenol/chloroform/isoamyl alcohol extraction. The obtained solutions including nucleic acids were treated with DNase I (Promega, WI, USA) at 37°C for 1 h to remove contaminated DNA. After removal of DNase I, the RNA pellets were dissolved with 20 μL MilliQ water.

RNA-seq analysis. One microgram of total RNA was used for library synthesis as follows. Ribosomal RNA was removed using RiboZero bacteria kit (Illumina, San Diego, CA, USA) following the manufacturer's protocol. Sequencing libraries were prepared by NEBNext mRNA library prep kit for Illumina (NEB, MA, USA) with the following modifications. The random hexamer primer was used for reverse transcription. After second strand synthesis, double stranded cDNA were fragmented to an average length of 300 bp using a Covaris S2 sonication system (Covaris, Woburn, CA, USA). One hundred cycles of paired-end sequencing were carried out using HiSeq2500 system according to the manufacturer's specifications (Illumina). After the sequencing reactions were complete, the Illumina analysis pipeline (CASAVA 1.8.0) was used to process the raw sequencing data. The RNA-Seq reads were trimmed using CLC Genomics Workbench ver. 9.5. with the following parameters: Phred quality score >30; Removing terminal 15 nucleotides from 5′ end and 2 nucleotides from 3' end; and removing truncated reads less than 30 nucleotides length. Trimmed reads were mapped to all the genes in *A. marina* 11017 chromosome and plasmids (accession number: NC_009925–NC_009934) using CLC Genomics Workbench ver. 9.5. (Qiagen, Germany) with the following parameters: Length fraction: 0.7; Similarity fraction: 0.9; Maximum number of hits for a read: 1 (or 10; in case to detect the averaged expression levels of highly homologous genes). The expression level of each gene was calculated by counting the mapped reads to each gene and were normalized by calculating the TPM values. Original sequence reads were deposited to the DRA/SRA database with the following accession numbers (DRR194261–DRR194266).

Real-time qPCR analysis. For cDNA preparation, RNA was reverse transcribed using random primers (PrimeScript RT reagent kit with gDNA eraser, Takara, Japan). Real-time qPCR was performed using THUNDERBIRD SYBR qPCR Mix (Toyobo, Japan) and the Thermal Cycler Dice Real Time System II (Takara). The expression level at each time point was normalized to the internal control (*rnpB*). The primers are listed in Supplementary Table S3.

Table 1. List of highly up-regulated 30 transcripts with *p*-value less than 0.01 under the orange light (OL) condition than that under the far-red light (FRL) condition.

Rank	genomic locus	locus_tag	old_locus_tag	Annotation	Fold change (OL/FRL)	P-value
1	pREB3	AM1_RS32450	AM1_C0090	hypothetical protein	1648.46	5.20E-15
2	pREB3	AM1_RS32640	AM1_C0146	DUF897 domain transmembrane protein	678.02	6.90E-17
3	pREB3	AM1_RS32830	-	hypothetical protein	298.41	2.48E-05
4	pREB3	AM1_RS32500	AM1_C0105	high light inducible protein	106.59	5.14E-14
5	pREB3	AM1_RS32550	AM1_C0120	hypothetical protein	97.79	2.53E-07
6	pREB3	AM1_RS32645	AM1_C0147	nitrogen regulatory protein P-II, putative	95.86	2.33E-16
7	pREB1	AM1_RS29185	AM1_A0082	conserved domain protein	95.51	8.58E-08
8	pREB6	AM1_RS36065	AM1_F0161	hypothetical protein	89.84	3.96E-11
9	pREB6	AM1_RS35915	AM1_F0130	streptomycin biosynthesis operon possible regulatory protein, putative	88.20	5.33E-07
10	pREB1	AM1_RS38260	AM1_A0059	conserved hypothetical protein	86.47	2.05E-11
11	pREB3	AM1_RS32535	AM1_C0117	fragment of phycocyanin subunit alpha	84.73	8.10E-19
12	pREB1	AM1_RS30280	AM1_A0354	RNA polymerase sigma-70 factor, putative	75.97	9.49E-09
13	pREB7	AM1_RS36630	AM1_G0114	photosystem II 12 kDa extrinsic protein PsbU	74.87	2.78E-05
14	pREB6	AM1_RS36135	AM1_F0176	RNA polymerase sigma-70 factor, putative	71.87	1.61E-06
15	pREB6	AM1_RS35840	AM1_F0112	hypothetical protein	70.47	6.65E-11
16	pREB5	AM1_RS34625	AM1_E00´7	hypothetical protein	66.90	3.00E-11
17	pREB1	AM1_RS29020	AM1_A0041	SAM-dependent methyltransferase, putative	66.78	1.58E-05
18	pREB5	AM1_RS34630	AM1_E00´9	hypothetical protein	65.43	9.87E-11
19	pREB1	AM1_RS30260	-	hypothetical protein	56.10	2.56E-04
20	pREB7	AM1_RS38160	AM1_G0173	FG-GAP repeat protein	53.11	7.99E-08
21	pREB6	AM1_RS36075	AM1_F0163	hypothetical protein	50.92	3.74E-06
22	pREB3	AM1_RS32545	AM1_C0119	CpcT protein, putative	49.49	4.31E-07
23	pREB5	AM1_RS34710	AM1_E0037	RNA polymerase sigma-70 factor	49.05	2.76E-06
24	pREB3	AM1_RS32455	AM1_C0092	phycobilisome rod-membrane linker polypeptice; CpcL	48.95	3.26E-11
25	pPEB5	AM1_RS34660	AM1_E0026	hypothetical protein	47.37	1.18E-13
26	pREB6	AM1_RS35845	AM1_F0113	two-component transcriptional regulator	46.74	1.01E-03
27	pREB1	AM1_RS29065	AM1_A0051	RNA-binding protein	45.64	3.65E-05
28	pREB1	AM1_RS29100	AM1_A0060	conserved hypothetical protein	44.73	3.96E-07
29	pREB1	AM1_RS29610	-	hypothetical protein	41.31	7.43E-04
30	pREB5	AM1_RS34610	AM1_E00´1	hypothetical protein	39.44	1.80E-20

Electron microscopy. Cells were harvested by two-step centrifugation at 4,000 rpm for 10 min and 5,000 rpm for 5 min (MX-305, TOMY). Cell pellets were frozen in a high-pressure freezing machine (EM PACT2, Leica Microsystems, Germany). The samples were transferred to 2% osmium tetroxide in dry acetone at –80°C, and freeze substituted at –80°C for more than 48 h. Subsequently, the samples were warmed gradually from –80 to –30°C over 5 h, held for 6 h at –30°C, then warmed again from –30 to 0°C over 3 h, and incubated for 2 h at 0°C (EM AFS2, Leica Microsystems). Then, the samples were washed three times with dry acetone at room temperature and infiltrated with increasing concentrations of low viscosity epoxy resin (Nisshin EM, Japan), and finally embedded. Ultrathin sections (60–80 nm) were cut with a diamond knife on an ultramicrotome (UC7, Leica Microsystems) and mounted on formvar-coated copper grids. The sections were stained with 4% uranyl acetate for 12 min and with lead citrate for 2 min, and then examined using a transmission electron microscope (JEM-1400, JEOL, Japan) at 80 kV.

Results

Spectral characteristics of the original strain of A. marina 11017

Although the original strain of *A. marina* 11017 just after isolation has accumulated PBS at a very low level, cultivation under the fluorescent lamp for a long period resulted in constitutive high accumulation of the PBS (Miyashita, personal communication). In order to reveal the native photoacclimation mechanism of *A. marina* 11017, we obtained the original strain of *A. marina* 11017, which accumulated the PBS at a low level (Fig. 1, gray line). We cultivated the original strain under an orange light condition for two weeks and compared its cellular absorption spectra with that under a far-red light condition (Fig. 1). Specific absorbance ratios (SARs) for both cells were calculated as the PBS absorption maximum at 613 nm divided by the photosynthetic reaction center absorption at 712 nm, providing a relative degree of PBS accumulation: 0.21 and 0.32 under far-red and orange light conditions, respectively. Judging by these values, cells under the orange light condition accumulated PBS by about 1.5-fold more than those under the far-red light condition. Notably, absorbance at 613 nm was relatively higher than that at 647 nm for cells under the orange light condition, whereas absorbance at 613 nm is comparable to that at 647 nm for cells under the far-red light condition.

Transcriptomic analysis

To comprehensively monitor transcriptional profiles responding to orange and far-red light exposures, we performed RNA-seq analyses using cells incubated under orange and far-red light conditions for 1 h. To compare the transcriptional levels, we calculated the TPM value for each gene. Because we did not monitor the transcriptional level under a normal white light condition, we were not able to judge whether a certain gene was induced or repressed in response to the monochromic light exposure. In this context, we relatively evaluated the gene expression profiles whether up-regulated or down-regulated in comparison with the sample exposed to the other monochromic light condition. As a result, up-regulated genes in response to the orange-light and far-red exposures (over a twice-higher expression level than the other light exposure) were calculated to be 540 and 244 genes, respectively (Fig. 2) with a *p*-value less than 0.01. Of these, the top 30 highly up-regulated genes for each light exposure are listed in Tables 1 and 2. Genes related to a PBS encod-

Table 2. List of highly up-regulated 30 transcripts with *p*-value less than 0.01under the far-red light (FRL) condition than that under the orange light (OL) condition.

Rank	genomic locus	locus_tag	old_locus_tag	Annotation	Fold change (FRL/OL)	P-value
1	pREB3	AM1_RS32910	AM1_C0220	phycobilisome degradation protein, nblA homolog	288.51	1.21E-08
2	chromosome	AM1_RS20780	AM1_4585	high light inducible protein	97.06	2.04E-15
3	chromosome	AM1_RS01325	AM1_0305	tRNA-Leu	83.67	2.66E-05
4	pREB3	AM1_RS33100	AM1_C0279	hypothetical protein	80.84	8.68E-03
5	chromosome	AM1_RS01330	AM1_0306	tRNA-Leu	63.93	1.55E-06
6	chromosome	AM1_RS01860	AM1_0429	rare lipoprotein A, putative	62.78	7.88E-78
7	chromosome	AM1_RS01310	AM1_0302	tRNA-Asn	59.64	2.16E-04
8	chromosome	AM1_RS01390	AM1_0322	tRNA-Arg	37.39	5.98E-04
9	chromosome	AM1_RS28665	AM1_6373	NAD(P)H dehydrogenase, subunit NdhF3 homolog	37.28	8.30E-10
10	chromosome	AM1_RS01255	AM1_0288	HNH endonuclease family protein	36.60	3.49E-06
11	chromosome	AM1_RS22690	AM1_5009	high light inducible protein	34.82	1.21E-22
12	chromosome	AM1_RS01315	AM1_0303	tRNA-Gln	32.77	2.39E-05
13	pREB3	AM1_RS33405	AM1_C0366	two-component sensor and regulator histidine kinase	32.09	6.11E-05
14	chromosome	AM1_RS01260	AM1_0289	conserved hypothetical protein	31.75	4.54E-06
15	chromosome	AM1_RS23080	AM1_5096	two-component transcriptional regulator	31.48	2.95E-36
16	chromosome	AM1_RS28660	AM1_6372	NAD(P)H dehydrogenase, subunit NdhD3 homolog	30.41	1.82E-09
17	pREB3	AM1_RS32240	AM1_C0040	hypothetical protein	30.08	1.42E-03
18	chromosome	AM1_RS07115	AM1_1594	high light inducible protein	28.37	5.46E-10
19	chromosome	AM1_RS01265	AM1_0290	hypothetical protein	24.79	3.50E-06
20	chromosome	AM1_RS14100	AM1_3103	folate/biopterin transporter, putative	23.36	4.13E-44
21	chromosome	AM1_RS14715	AM1_3236	PGR5 protein involved in cyclic electron flow	20.12	3.65E-10
22	chromosome	AM1_RS14095	AM1_3102	retinal pigment epithelial membrane protein, putative	19.84	2.19E-32
23	chromosome	AM1_RS04405	AM1_0990	hypothetical protein	18.67	3.05E-35
24	chromosome	AM1_RS06235	AM1_1403	ABC-1 family protein	18.35	5.84E-42
25	chromosome	AM1_RS20790	AM1_4588	PGR5 protein involved in cyclic electron flow	17.76	1.05E-05
26	chromosome	AM1_RS21125	AM1_4659	fatty acid desaturase (Delta(12) desaturase)	16.86	1.32E-31
27	chromosome	AM1_RS01350	AM1_0310	hypothetical protein	16.68	2.40E-05
28	chromosome	AM1_RS10555		hypothetical protein	15.93	1.20E-34
29	pPEB7	AM1_RS36550	AM1_G0093	hypothetical protein	15.35	8.65E-03
30	pREB3	AM1_RS32940	AM1_C0232	hypothetical protein	14.84	1.37E-04

Table 3. Expression profiles of the *cpcA1*, *cpcB1*, *cpcA2* and *cpcB2*.

Name	genomic locus	locus_tag	old_locus_tag	Gene product	Fold change (OL/FRL)	P-value
cpcA1	pREB3	AM1_RS32480 or AM1_RS32800	AM1_C0099 or AM1_C0191	CpcA: phycocyanin alpha subunit	18.97	3.94E-02
cpcB1	pREB3	AM1_RS32485 or AM1_RS32805	AM1_C0100 or AM1_C0192	CpcB: phycocyanin alpha subunit	19.69	4.17E-02
cpcA2	pREB3	AM1_RS32470 or AM1_RS32880	AM1_C0096 or AM1_C0213	CpcA: phycocyanin alpha subunit	1.66	2.99E-02
cpcB2	pREB3	AM1_RS32475 or AM1_RS32875	AM1_C0098 or AM1_C0212	CpcB: phycocyanin beta subunit	1.92	7.08E-02

Table 4. Expression profiles of the allophycocyanin genes.

genomic locus	locus_tag	old_locus_tag	Annotation	Fold change (OL/FRL)	P-value	TPM value (FRL)	TPM value (OL)
chromosome	AM1_RS06940	AM1_1558	allophycocyanin alpha subunit ApcA	1.08	1.00E+00	3.17	3.41
chromosome	AM1_RS20255	AM1_4469	allophycocyanin alpha subunit ApcA	2.62	1.13E-06	25.58	63.52
chromosome	AM1_RS26260	AM1_5810	allophycocyanin alpha subunit ApcA	2.22	1.53E-03	3.71	7.14
chromosome	AM1_RS10705	AM1_2376	allophycocyanin beta subunit ApcB	1.66	1.10E-02	356.73	603.79

ing fragment of *cpcA* (probably pseudogene, AM1_C0117), *cpcT* (AM1_C0119) and *cpcL* (AM1_C0092) and sigma factor genes encoded on pREB1 (AM1_A0354), pREB5 (AM1_E0037) and pREB6 (AM1_F0176) were highly up-regulated under the orange light condition, whereas *nblA* gene for PBS degradation (AM1_C0220), genes related to NDH1 complex genes, *ndhF3* (AM1_6373) and *ndhD3* (AM1_6372) and genes homologous to PGR5 (AM1_3236 and AM1_4588) were highly up-regulated under the far-red light condition.

CpcB and CpcA are the phycocyanobilin-binding phycocyanin proteins to absorb the orange light and to transfer the absorbed energy to the photosystems, whose transcripts are listed in the highly up-regulated 100 transcripts under the orange light condition (Supplementary Table S1). Notably, *A. marina* 11017 encodes CpcB and CpcA for four loci on the pREB3 plasmid as operons: AM1_C0098/AM1_C0096, AM1_C0212/AM1_C0213, AM1_C0100/AM1_C0099 and AM1_C0192/AM1_C0191. AM1_C0098 operon is almost identical to AM1_C0212 operon (1 bp mismatch for *cpcB* genes and identical for *cpcA* genes), whereas AM1_C0100 operon is almost identical to AM1_C0192 operon (2 bp mismatch for *cpcB* genes and identical for *cpcA* genes). In this paper, we named AM1_C0100, AM1_C0192, AM1_C0098 and AM1_C0212 operons as *cpcBA1a*, *cpcBA1b*, *cpcBA2a* and *cpcBA2b* operons, respectively. In such a situation, read sequences mapped on both identical regions were not counted as an individual expression by the conventional method applied in the present study. Thus, we re-mapped the sequences without distinguishing these homologous genes. As a result, *cpcB1* (AM1_C0100/AM1_C0192) and

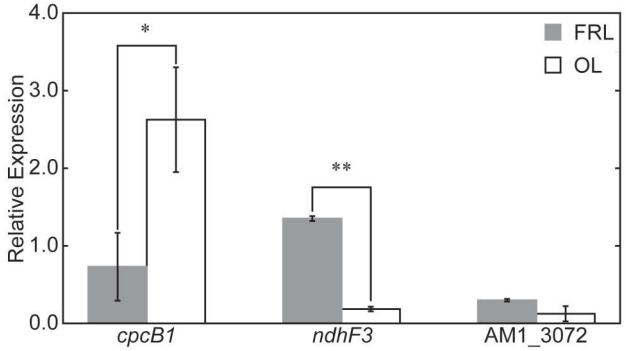

Fig. 3. Bar graphs showing relative expression levels for *cpcB1* (AM1_C0100/AM1_C0192), *ndhF3* (AM1_6373) and AM1_3072 determined by Real-Time qPCR analysis under the far-red (FRL) and orange (OL) light conditions.

$n = 3$. All data were presented as mean ± SD. $*P < 0.05$, $**P < 0.01$ (paired Student's *t*-test).

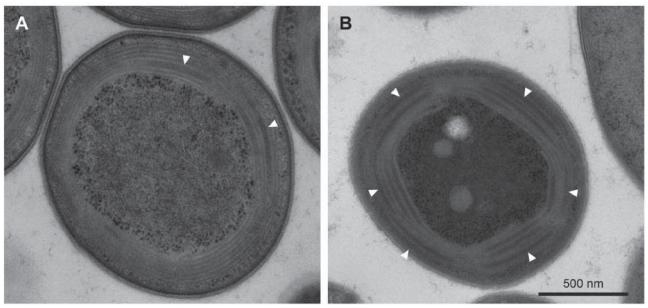

Fig. 4. Electron microscopy of cells under far-red and orange light conditions.

A. Cells under far-red light condition. B. Cells under orange light condition. Arrowheads, phycobilisomes.

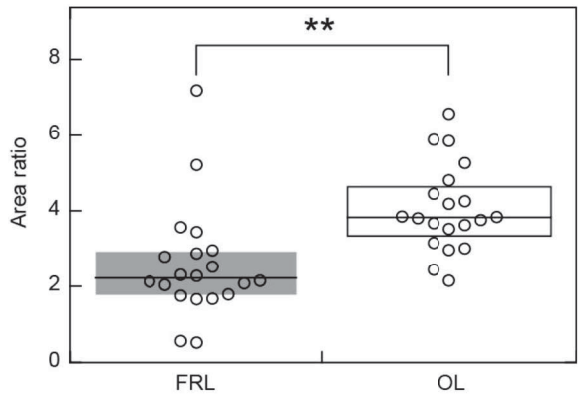

Fig. 5. Area ratio of the PBS region relative to the whole cell area under the far-red (FRL) and orange (OL) light conditions.

$n = 20$. $**P < 0.01$ (paired Student's *t*-test).

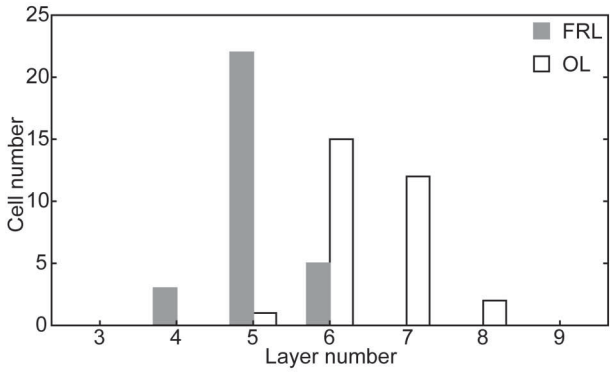

Fig. 6. Histogram of numbers of the thylakoid membrane layers under far-red (FRL) and orange (OL) light conditions.

cpcA1 (AM1_C0099/AM1_C0191) were highly up-regulated under the orange light condition, whereas *cpcB2* (AM1_C0098/AM1_C0212) and *cpcA2* (AM1_C0096/AM1_C0213) were almost constitutively expressed under both light conditions (Table 3).

A. marina 11017 encoded membrane-anchoring CpcL proteins for three loci on the pREB3 plasmid: AM1_C0092, AM1_C0102 and AM1_C0203 (named *cpcL1*, *cpcL2* and *cpcL3*, respectively). Notably, only *cpcL1* was highly up-regulated under the orange light condition, whereas *cpcL2* and *cpcL3* showed slightly higher up-regulation under the orange light condition than that under the far-red light condition.

To quantitatively verify the differential expression patterns observed by the RNA-seq analyses, we selected some genes to analyze by quantitative Real-Time PCR: *cpcB1*, *ndhF3* and AM1_3072 encoding Zn ABC transporter and showing a constitutive expression (Fig. 3). We used *rnpB* gene (AM1_6418) for an internal standard. As a result, consistent with the RNA-seq analysis, *cpcB1* was highly up-regulated under the orange light condition, whereas *ndhF3* was highly up-regulated under the far-red light condition. Conversely, AM1_3072 was constitutively expressed under both conditions. These results ensure that the differential expression profile obtained by the RNA-seq analysis is reliable.

Observation by electron microscopy

We performed morphological observations by electron microscopy to reveal cellular processes responsive to the orange and far-red light exposures. We observed the cells incubated under the orange and far-red light conditions for 14 days, which is enough for PBS accumulation under the orange light condition (Fig. 4). Thylakoid membranes were present at the periphery of cells as concentric multilayers with two types of cytoplasmic space: space with a low electron density, and space with a high electron density (white arrowheads). Because PBS is a supercomplex of megadalton sitting on the thylakoid surface, the electron density space between the thylakoid membranes should be filled with such PBS, which is consistent with the previous observations (Chen et al., 2009; Hu et al., 1999). We calculated the ratios of these areas to the total cell areas for 20 cells under both light conditions: 4.06% and 2.58% for the orange and far-red light acclimated cells, respectively (Fig. 5). Namely, cells under the orange light condition showed a significantly higher PBS accumulation than those under the far-red light condition. This observation is consistent with the cell absorption spectra and the transcriptional profiles described above.

Next, we calculated the number of the thylakoid membrane layers within the cells. Figure 6 shows a histogram

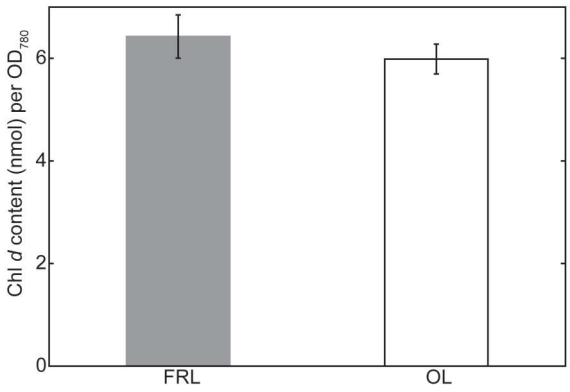

Fig. 7. Chlorophyll *d* contents under the far-red and orange light conditions.

$n = 3$. All data were presented as mean ± SD.

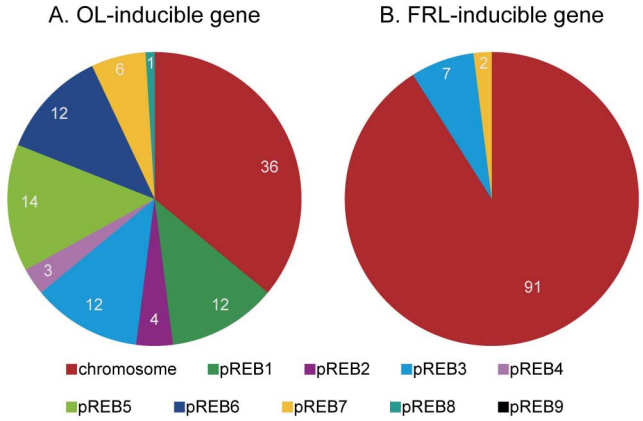

Fig. 8. Pie charts of highly up-regulated 100 transcripts with *P*-value < 0.01 in RNA-seq profiles.

Number of genes encoded on chromosome or each plasmid responsive to orange (A) and far-red (B) light exposures.

of these numbers. Most cells under the orange light condition contained 6–7 thylakoid membrane layers, whereas most cells under the far-red light condition contained 5 thylakoid membrane layers. In conclusion, the cells under the orange light condition possess more thylakoid membrane layers than those under the far-red light condition (Fig. 6). Because the PBS absorbance in the orange light region is largely lower than that in the far-red light region even under the orange light conditions (Fig. 1B), cultivation with the same light intensity of 10 μmol photons m^{-2} s^{-1} led to a situation, in which cells recognize orange light as having a relatively lower light intensity than the far-red light. Based on this assumption, the increase in the thylakoid membrane layers under the orange light condition can be regarded as an acclimation process to harvest more light energy. To verify this assumption, we measured the chlorophyll *d* contents under the orange and far-red light conditions, but, unexpectedly, there is no significant difference between these chlorophyll *d* contents (Fig. 7). In this context, it is of note that the PBS supercomplexes were partly localized on the thylakoid membrane layers (Fig. 4). We thus speculate that an increase of the thylakoid membrane layers under the orange light condition may be advantageous for efficient orange light harvesting by the PBS.

Discussion

Chromatic acclimation responsive to orange light

The cellular absorption spectra, transcriptomic profiles and microscopic observations we have obtained are consistent with each other and demonstrate that PBS highly accumulates under an orange light condition (Fig. 1B, Figs. 2–5). Electron microscopy results clearly show that the PBS area relative to the total cell area under an orange light condition was significantly higher than that under a far-red light condition (Figs. 4 and 5). The PBS of *A. marina* 11017 exceptionally lacks the core component and contains only the rod component, which is composed of four disks (Chen et al., 2009). Because gap lengths of the thylakoid membrane under both orange and far-red light conditions were comparable to each other (Fig. 4), the increase in PBS contents under the orange light condition is mainly due to an increase in rod number, but not an extension of rod length. In the present study, we monitored the expression profiles 1 h after a monochromic light exposure, while we monitored the cell absorption spectra 14 days after the monochromic light cultivation. It was shown that chromatic acclimation takes a long time (~1 week), but a quick transcriptional response (2–4 hours) is achieved in the cyanobacterium *Fremyella diplosiphon* (Federspiel and Grossman, 1990). We also observed a similar tendency to show a quick transcriptional response and a slow chromatic acclimation in the other cyanobacterium *A. marina* 11017.

Transcriptome analysis clarified that the *cpcBA1* operon showed a higher up-regulation under an orange light condition than that under a far-red light condition, whereas *cpcBA2* is constitutively expressed under both orange and far-red light conditions (Table 3). On the other hand, cellular absorbance spectral measurement revealed that there are two absorption peaks at 613 nm and 647 nm for PBS, and the shorter peak is more prominent than the longer peak under the orange light condition, but not under the far-red light condition (Fig. 1B). These facts suggest that the phycocyanin disks composed of CpcBA1 and CpcBA2 correspond to the shorter and longer peaks, respectively. These two homologous proteins show about a 70% identity with each other. These sequence alterations may cause distinctive spectral properties. Among the four disks of the PBS rod, three disks are homohexamers composed of only phycocyanins, whereas one disk at the bottom is thought to be a heterohexamer composed of phycocyanin and allophycocyanin (Chen et al., 2002, 2009; Golub et al., 2017; Gryliuk et al., 2014; Hu et al., 1999; Marquardt et al., 1997). A recent study, however, reported that the purified PBS contained allophycocyanin at only a trace level (Bar-Zvi et al., 2018). Based on our transcriptional data, allophycocyanin genes, *apcA* (AM1_1158, AM1_4469, AM1_5810) and *apcB* (AM1_2376), are almost constitutively expressed under both orange and far-red light conditions with relatively low TPM values (Table 3), indicating that the allophycocyanin content within the PBS complex should be fixed under these conditions,

or the allophycocyanin may form some apparatus independent of the canonical PBS complex. Taken together, *A. marina* 11017 is likely to show orange light-responsive chromatic acclimation to increase the PBS content and to change the composition of the two phycocyanin variants.

Various responses to far-red light

The top 1 up-regulated gene under a far-red light condition was the *nblA* gene that is involved in the PBS degradation pathway (Collier and Grossman, 1994). Because almost no transcripts have been detected for the sample under an orange light condition, remarkable up-regulation of this gene may be detected. Although in this study, it is difficult to judge whether expression of the *nblA* gene is induced under the far-red light condition, or repressed under the orange light condition, a relatively low expression under the orange light condition is consistent with the fact that the orange light promotes PBS accumulation.

In contrast with the orange light exposure, a far-red light exposure mimics a relatively high light environment for *A. marina* 11017 cells, which is supported by the fact that expressions of many high light inducible genes were up-regulated under the far-red light condition (Table 2 and Supplementary Table S2). In such a situation, a rate-limiting steps in photosynthesis are dark-reaction processes. In this context, it is of note that expressions of CCM (CO_2 concentrating mechanism)—related genes, *ndhF3*, *ndhD3*, *cupA* and *cupS* (AM1_6373, AM1_6372, AM1_6371 and AM1_6370) are highly up-regulated by far-red light exposure (Table 2 and Table S2). The former two genes are listed in the highly up-regulated 30 transcripts, while the latter two genes are listed in the highly up-regulated 100 transcripts. These genes have been identified to be highly expressed under low CO_2 conditions in a model cyanobacterium (Shibata et al., 2001; Zhang et al., 2004). The transcriptional up-regulation of these genes under a far-red light condition should lead to the efficient incorporation of CO_2, and so can be regarded as an acclimation process to resolve the rate-limiting dark-reaction processes.

Furthermore, we found that expressions of genes related to the cyclic electron transport were up-regulated under a far-red light condition. In addition to the PGR5-like genes (AM1_3236 and AM1_4588) that are listed in the highly up-regulated 30 transcripts (Table 2), expressions of one more PGR5-like gene (AM1_1597), flavodiiron genes (AM1_1384 and AM1_1386), and *ndhD1/F1* genes (AM1_2497 and AM1_2496), were up-regulated and are listed in the highly up-regulated 100 transcripts (Table S2). All these genes have been reported to be involved in the cyclic electron transport in the model cyanobacterium *Synechocystis* sp. PCC 6803 (Allahverdiyeva et al., 2015a, b; Battchikova et al., 2011; Yeremenko et al., 2005). Because monochromic far-red light preferentially excites the PS I, induction of these genes may contribute to the consumption of the resultant excessive electron from PS I.

Recently, the Chen group has reported that far-red light exposure resulted in transcriptional up-regulation of extracellular polysaccharide synthetic genes and cell aggregation via biofilm formation in *A. marina* 11017 (Hernández-Prieto et al., 2018). Conversely, we could not detect transcriptional up-regulation of these genes under the far-red light condition, probably because of a difference in the experimental conditions. We observed a short-term response (1 h) to 10 μmol photons m^{-2} s^{-1} in the present study, whereas the Chen group observed a long-term response (one week) to 20 μmol photons m^{-2} s^{-1} (Hernández-Prieto et al., 2018). Long-term higher light exposure should excessively trigger a photosynthetic reaction in comparison with short-term lower light exposure, which may induce the cell aggregation to avoid photoinhibition by self-shading.

Potential regulatory mechanism

We recently discovered that some CBCR photoreceptors (AM1_1557, AM1_C0023 and AM1_6305) from *A. marina* 11017 covalently bound not only PCB, but also BV and the BV-binding ones showed far-red/orange reversible photoconversion (Fushimi et al., 2016, 2019; Narikawa et al., 2015). The far-red/orange reversibility of these photoreceptors corresponds well with the far-red/orange-responsive chromatic acclimation addressed in the present study. Although these proteins possess two-component His kinase and response regulator domains as a signal output, we could not detect clear cognate transcriptional regulators near genes encoding these photoreceptors. Because there have been no reports to knock out target genes in *A. marina* 11017 to date, the detailed regulatory mechanism of this chromatic acclimation should be addressed as future work.

Notably, all phycocyanin genes of *A. marina* 11017 are encoded on a specific plasmid, pREB3, whereas allophycocyanin *apcA* and *apcB* genes are encoded on a main chromosome (Swingley et al., 2008). The closely related species *A.* 5410 has been reported to lack the PBS absorbance and its draft genome contains *apcA* and *apcB* genes, but no phycocyanin genes (Miller et al., 2005; Yoneda et al., 2016). We further confirmed that no genes orthologous to the other genes encoded on *A. marina* 11017 pREB3 were detected from the draft genome of *A.* 5410. These facts strongly indicate that *A.* 5410 do not possess the pREB3 plasmid. There are two possibilities: *A. marina* 11017 acquired the pREB3 plasmid, or *A.* 5410 lost the corresponding plasmid. In this context, it should be noted that both PBS, and photosystem structures of *Acaryochloris* genus are quite unique among known cyanobacterial species. Thus, it is unlikely that laterally acquired phycocyanins functionally connect to the photosystems in *A. marina* 11017. Namely, *Acaryochloris* genus may employ a strategy to put phycocyanin-related genes, into the specific pREB3 plasmid, which enables them to specifically regulate their expression, or in some cases to discard these genes depending on their habitat.

We further found that all of the highly up-regulated 30 transcripts under the orange light condition were encoded on the plasmids, while most of those under a far-red light condition were encoded on the main chromosome (Tables 1 and 2). To examine this trend in detail, we constructed pie charts of the highly up-regulated 100 transcripts for both light conditions (Fig. 8). Although genes encoded on the pREB3 were up-regulated under both light conditions,

many more genes on the pREB3 were up-regulated under the orange light condition than those under the far-red light condition. The up-regulation of the pREB3 genes under the orange light condition corresponds well to the presence of the PBS-related genes in this plasmid, as mentioned above. On the other hand, a large number of genes encoded on pREB1, pREB5 and pREB6 were up-regulated under the orange light condition, but not under the far-red light condition at all. It is of note that sigma factor genes encoded on these plasmids showed prominent expression induction under the orange light condition (Table 1). These sigma factors possibly contribute to the global induction of gene expression encoded on these plasmids. The up-regulated genes on these plasmids, however, mostly encode hypothetical proteins. Unraveling the physiological function of these proteins will provide insights into the acclimation strategy to the orange light environment of *A. marina* 11017.

Acknowledgments

We appreciate the support of Mayumi Wakazaki (RIKEN CSRS), Katsuyuki Uematsu (Marine Works Japan Ltd.) and Naeko Shinozaki-Narikawa (RIKEN CSRS) for electron microscopy experiments. We also thank NITE Biological Research Center for providing the cyanobacterial strain. This study was also funded by a Cooperative Research Grant of the Genome Research for BioResource, NODAI Genome Research Center, Tokyo University of Agriculture.

Supplementary Materials

Supplementary tables are available in our J-STAGE site (http://www.jstage.jst.go.jp/browse/jgam).

References

Allahverdiyeva, Y., Isojärvi, J., Zhang, P., and Aro, E.-M. (2015a) Cyanobacterial oxygenic photosynthesis is protected by flavodiiron proteins. *Life*, **5**, 716–743.

Allahverdiyeva, Y., Suorsa, M., Tikkanen, M., and Aro, E.-M. (2015b) Photoprotection of photosystems in fluctuating light intensities. *J. Exp. Bot.*, **66**, 2427–2436.

Bar-Zvi, S., Lahav, A., Harris, D., Niedzwiedzki, D. M., Blankenship, R. E. et al. (2018) Structural heterogeneity leads to functional homogeneity in *A. marina* phycocyanin. *Biochim. Biophys. Acta Bioenerg.*, **1859**, 544–553.

Battchikova, N., Eisenhut, M., and Aro, E.-M. (2011) Cyanobacterial NDH-1 complexes: novel insights and remaining puzzles. *Biochim. Biophys. Acta*, **1807**, 935–944.

Chen, M., Quinnell, R. G., and Larkum, A. W. D. (2002) The major light-harvesting pigment protein of *Acaryochloris marina*. *FEBS Lett.*, **514**, 149–152.

Chen, M., Floetenmeyer, M., and Bibby, T. S. (2009) Supramolecular organization of phycobiliproteins in the chlorophyll *d*-containing cyanobacterium *Acaryochloris marina*. *FEBS Lett.*, **583**, 2535–2539.

Chen, M., Schliep, M., Willows, R. D., Cai, Z.-L., Neilan, B. A. et al. (2010) A red-shifted chlorophyll. *Science*, **329**, 1318–1319.

Chen, M., Li, Y., Birch, D., and Willows, R. D. (2012) A cyanobacterium that contains chlorophyll *f*—a red-absorbing photopigment. *FEBS Lett.*, **586**, 3249–3254.

Collier, J. L. and Grossman, A. R. (1994) A small polypeptide triggers complete degradation of light-harvesting phycobiliproteins in nutrient-deprived cyanobacteria. *EMBO J.*, **13**, 1039–1047.

Duxbury, Z., Schliep, M., Ritchie, R. J., Larkum, A. W. D., and Chen, M. (2009) Chromatic photoacclimation extends utilisable photosynthetically active radiation in the chlorophyll *d*-containing cyanobacterium, *Acaryochloris marina*. *Photosynth. Res.*, **101**, 69–75.

Enomoto, G., Nomura, R., Shimada, T., Ni-Ni-Win, Narikawa, R. et al. (2014) Cyanobacteriochrome SesA is a diguanylate cyclase that induces cell aggregation in *Thermosynechococcus*. *J. Biol. Chem.*, **289**, 24801–24809.

Enomoto, G., Ni-Ni-Win, Narikawa, R., and Ikeuchi, M. (2015) Three cyanobacteriochromes work together to form a light color-sensitive input system for c-di-GMP signaling of cell aggregation. *Proc. Natl. Acad. Sci. USA*, **112**, 8082–8087.

Federspiel, N. A. and Grossman, A. R. (1990) Characterization of the light-regulated operon encoding the phycoerythrin-associated linker proteins from the cyanobacterium *Fremyella diplosiphon*. *J. Bacteriol.*, **172**, 4072–4081.

Fushimi, K. and Narikawa, R. (2019) Cyanobacteriochromes: photoreceptors covering the entire UV-to-visible spectrum. *Curr. Opin. Struct. Biol.*, **57**, 39–46.

Fushimi, K., Nakajima, T., Aono, Y., Yamamoto, T., Ni-Ni-Win et al. (2016) Photoconversion and fluorescence properties of a red/green-type cyanobacteriochrome AM1_C0023g2 that binds not only phycocyanobilin but also biliverdin. *Front. Microbiol.*, **7**, 588.

Fushimi, K., Miyazaki, T., Kuwasaki, Y., Nakajima, T., Yamamoto, T. et al. (2019) Rational conversion of chromophore selectivity of cyanobacteriochromes to accept mammalian intrinsic biliverdin. *Proc. Natl. Acad. Sci. USA*, **116**, 8301–8309.

Gan, F. and Bryant, D. A. (2015) Adaptive and acclimative responses of cyanobacteria to far-red light. *Environ. Microbiol.*, **17**, 3450–3465.

Gan, F., Zhang, S., Rockwell, N. C., Martin, S. S., Lagarias, J. C. et al. (2014) Extensive remodeling of a cyanobacterial photosynthetic apparatus in far-red light. *Science*, **345**, 1312–1317.

Golub, M., Combet, S., Wieland, D. C. F., Soloviov, D., Kuklin, A. et al. (2017) Solution structure and excitation energy transfer in phycobiliproteins of *Acaryochloris marina* investigated by small angle scattering. *Biochim. Biophys. Acta Bioenerg.*, **1858**, 318–324.

Gryliuk, G., Rätsep, M., Hildebrandt, S., Irrgang, K.-D., Eckert, H.-J. et al. (2014) Excitation energy transfer and electron-vibrational coupling in phycobiliproteins of the cyanobacterium *Acaryochloris marina* investigated by site-selective spectroscopy. *Biochim. Biophys. Acta*, **1837**, 1490–1499.

Hernández-Prieto, M. A., Li, Y., Postier, B. L., Blankenship, R. E., and Chen, M. (2018) Far-red light promotes biofilm formation in the cyanobacterium *Acaryochloris marina*. *Environ. Microbiol.*, **20**, 535–545.

Hirose, Y., Narikawa, R., Katayama, M., and Ikeuchi, M. (2010) Cyanobacteriochrome CcaS regulates phycoerythrin accumulation in *Nostoc punctiforme*, a group II chromatic adapter. *Proc. Natl. Acad. Sci. USA*, **107**, 8854–8859.

Hu, Q., Marquardt, J., Iwasaki, I., Miyashita, H., Kurano, N. et al. (1999) Molecular structure, localization and function of biliproteins in the chlorophyll *a/d* containing oxygenic photosynthetic prokaryote *Acaryochloris marina*. *Biochim. Biophys. Acta*, **1412**, 250–261.

Kehoe, D. M. and Grossman, A. R. (1996) Similarity of a chromatic adaptation sensor to phytochrome and ethylene receptors. *Science*, **273**, 1409–1412.

Marquardt, J., Senger, H., Miyashita, H., Miyachi, S., and Mörschel, E. (1997) Isolation and characterization of biliprotein aggregates from *Acaryochloris marina*, a *Prochloron*-like prokaryote containing mainly chlorophyll *d*. *FEBS Lett.*, **410**, 428–432.

Miller, S. R., Augustine, S., Olson, T. L., Blankenship, R. E., Selker, J. et al. (2005) Discovery of a free-living chlorophyll *d*-producing cyanobacterium with a hybrid proteobacterial/cyanobacterial small-subunit rRNA gene. *Proc. Natl. Acad. Sci. USA*, **102**, 850–855.

Miyashita, H., Ikemoto, H., Kurano, N., Adachi, K., Chihara, M. et al. (1996) Chlorophyll *d* as a major pigment. *Nature*, **383**, 402.

Narikawa, R., Suzuki, F., Yoshihara, S., Higashi, S.-I., Watanabe, M. et al. (2011) Novel photosensory two-component system (PixA-NixB-NixC) involved in the regulation of positive and negative phototaxis of cyanobacterium *Synechocystis* sp. PCC 6803. *Plant Cell Physiol.*, **52**, 2214–2224.

Narikawa, R., Nakajima, T., Aono, Y., Fushimi, K., Enomoto, G. et al. (2015) A biliverdin-binding cyanobacteriochrome from the chlorophyll *d*-bearing cyanobacterium *Acaryochloris marina*. *Sci. Rep.*, **5**, 7950.

Savakis, P., De Causmaecker, S., Angerer, V., Ruppert, U., Anders, K. et al. (2012) Light-induced alteration of c-di-GMP level controls

motility of *Synechocystis* sp. PCC 6803. *Mol. Microbiol*., **85**, 239–251.

Shibata, M., Ohkawa, H., Kaneko, T., Fukuzawa, H., Tabata, S. et al. (2001) Distinct constitutive and low-CO_2-induced CO_2 uptake systems in cyanobacteria: genes involved and their phylogenetic relationship with homologous genes in other organisms. *Proc. Natl. Acad. Sci. USA*, **98**, 11789–11794.

Song, J.-Y., Cho, H. S., Cho, J.-I., Jeon, J.-S., Lagarias, J. C. et al. (2011) Near-UV cyanobacteriochrome signaling system elicits negative phototaxis in the cyanobacterium *Synechocystis* sp. PCC 6803. *Proc. Natl. Acad. Sci. USA*, **108**, 10780–10785.

Swingley, W. D., Chen, M., Cheung, P. C., Conrad, A. L., Dejesa, L. C. et al. (2008) Niche adaptation and genome expansion in the chlorophyll *d*-producing cyanobacterium *Acaryochloris marina*. *Proc. Natl. Acad. Sci. USA*, **105**, 2005–2010.

Watabe, K., Mimuro, M., and Tsuchiya, T. (2015) Establishment of the forward genetic analysis of the chlorophyll *d*-dominated cyanobacterium *Acaryochloris marina* MBIC 11017 by applying in vivo transposon mutagenesis system. *Photosynth. Res*., **125**, 255–265.

Watanabe, M. and Ikeuchi, M. (2013) Phycobilisome: architecture of a light-harvesting supercomplex. *Photosynth. Res*., **116**, 265–276.

Watanabe, M., Semchonok, D. A., Webber-Birungi, M. T., Ehira, S., Kondo, K. et al. (2014) Attachment of phycobilisomes in an antenna-photosystem I supercomplex of cyanobacteria. *Proc. Natl. Acad. Sci. USA*, **111**, 2512–2517.

Wiltbank, L. B. and Kehoe, D. M. (2016) Two cyanobacterial photoreceptors regulate photosynthetic light harvesting by sensing teal, green, yellow, and red light. *MBio*, **7**, e02130-15.

Yang, Y., Lam, V., Adomako, M., Simkovsky, R., Jakob, A. et al. (2018) Phototaxis in a wild isolate of the cyanobacterium *Synechococcus elongatus*. *Proc. Natl. Acad. Sci. USA*, **115**, E12378–E12387.

Yeremenko, N., Jeanjean, R., Prommeenate, P., Krasikov, V., Nixon, P. J. et al. (2005) Open reading frame ssr2016 is required for antimycin A-sensitive photosystem I-driven cyclic electron flow in the cyanobacterium *Synechocystis* sp. PCC 6803. *Plant Cell Physiol*., **46**, 1433–1436.

Yoneda, A., Wittmann, B. J., King, J. D., Blankenship, R. E., and Dantas, G. (2016) Transcriptomic analysis illuminates genes involved in chlorophyll synthesis after nitrogen starvation in *Acaryochloris* sp. CCMEE 5410. *Photosynth. Res*., **129**, 171–182.

Yoshihara, S., Suzuki, F., Fujita, H., Geng, X. X., and Ikeuchi, M. (2000) Novel putative photoreceptor and regulatory genes required for the positive phototactic movement of the unicellular motile cyanobacterium *Synechocystis* sp. PCC 6803. *Plant Cell Physiol*., **41**, 1299–1304.

Zhang, P., Battchikova, N., Jansen, T., Appel, J., Ogawa, T. et al. (2004) Expression and functional roles of the two distinct NDH-1 complexes and the carbon acquisition complex NdhD3/NdhF3/CupA/Sll1735 in *Synechocystis* sp. PCC 6803. *Plant Cell*, **16**, 3326–3340.

Zhao, C., Gan, F., Shen, G., and Bryant, D. A. (2015) RfpA, RfpB, and RfpC are the master control elements of far-red light photoacclimation (FaRLiP). *Front. Microbiol*., **6**, 1303.